# Large Surface Charge Density Oscillations Induced by Subsurface Phonon Resonances

V. Chis,[1,2] B. Hellsing,[3,4] G. Benedek,[2,4] M. Bernasconi,[2] E. V. Chulkov,[4] and J. P. Toennies[5]

[1]*Department of Physics, University of Gothenburg, Fysikgården 6B, S-412 96 Göteborg, Sweden*
[2]*Dipartimento di Scienza dei Materiali, Universitá di Milano-Bicocca, Via Cozzi 53, 20125 Milano, Italy*
[3]*Department of Physics, Göteborgs University, Fysikgården 6B, S-412 96 Göteborg, Sweden*
[4]*Donostia International Physics Center (DIPC), 20018 Donostia/San Sebastian, Spain*
[5]*Max-Planck-Institut für Dynamik und Selbstorganization, Bunsenstrasse 19, 37073 Göttingen, Germany*
(Received 28 July 2008; published 14 November 2008)

A density functional perturbation theory study of Cu(111) surface dynamics and phonon-induced surface charge density (SCD) oscillations shows that the subsurface phonon resonances such as $S_3$, first predicted by embedded-atom methods, trigger large SCD charge-density oscillations, thus explaining the large helium atom scattering intensity from the anomalous longitudinal resonance found in most metal surfaces. The strong coupling between certain phonons and SCD oscillations is shown to have implications in inelastic electron tunneling spectroscopy and other manifestations of electron-phonon interactions at metal surfaces.

There are common features characterizing all metal surfaces which originate from the redistribution of surface electronic charge with respect to the charge density in the bulk. Textbook examples are the relaxation of the surface atomic layers and a surface-dependent work function [1]. Another common feature is the existence of a surface acoustic phonon resonance (hereafter termed $S_3$) [2], not predicted by the continuum theory [3] and first observed by inelastic Helium atom scattering (HAS) in noble metal surfaces [4,5]. The $S_3$ dispersion curve is clearly detached from the lower edge of the longitudinal acoustic (LA) bulk phonon band, but at large wave-vectors, its frequency is significantly softer than the LA bulk edge and was therefore referred to as an anomalous longitudinal resonance. Most of these observations have been confirmed and extended by electron energy loss spectroscopy (EELS) [2,6–8].

Earlier calculations by Nelson *et al.* [9] with the embedded atom method (EAM) of Cu(111) and Ag(111) surface dynamics revealed that the $S_3$ resonance originates from an avoided crossing of the longitudinal acoustic mode with a 2nd-layer surface optical mode, leading to an exchange of characters at large wave vectors. This explanation raised, however, the problem of how HAS, which is a strictly surface-sensitive probe, can reveal a 2nd-layer resonance with intensities often largely exceeding those of Rayleigh waves (RW), especially in less densely packed surfaces like Cu(001) [10] and Cu(110) [11]. It was suggested, on the basis of a multipole-expansion model [12], that certain surface modes, though having a negligible shear-vertical (SV) amplitude in the surface layer, can nevertheless induce large surface charge density (SCD) oscillations and therefore large inelastic HAS amplitudes [13]. He atoms are scattered by the SCD oscillations about 3 Å above the first atomic layer, whereas electrons in the

inelastic impact regime are scattered by atom core displacements in the first few surface layers. Thus, (i) HAS intensities carry direct information on the SCD oscillations associated with surface phonons and ultimately on the surface electron-phonon ($e$-$p$) interaction, and (ii) certain surface modes peculiar to metal surfaces like the $S_3$ resonance trigger large SCD oscillations and must therefore play a major role in important manifestations of the $e$-$p$ interaction such as surface electron lifetimes [14] and inelastic electron tunneling spectroscopy (IETS) [15].

To substantiate these arguments, we present new HAS data exploring the $S_3$ branch of Cu(111) in the avoided-crossing region, and a theoretical study of surface dynamics and phonon-induced SCD oscillations based on density-functional perturbation theory (DFPT) [16]. The calculations, besides confirming the early EAM analysis as regards the nature of the $S_3$ resonance [9], yield the remarkable result that the $S_3$ resonance, albeit localized on the 2nd layer, causes comparatively large SCD oscillations, hinting for a strong coupling of this resonance to surface electronic states.

A selection of new HAS energy-transfer spectra measured along the $\langle 11\bar{2}\rangle$ direction at different incident angles $\Theta_i$ in a 90° scattering geometry, for an incident energy $E_i = 35.3$ meV and surface temperature $T_s = 160$ K are reported in Fig. 1(a). The comparatively small elastic peak ($E$), less than $10^{-5}$ times the elastic peak intensity $I_{00}$, certifies the good quality of the surface. The data points in the energy-wave vector plane, corresponding to the inelastic peaks are plotted in Fig. 1(b) together with previous HAS [5] and EELS [6,7] data. Besides the $S_3$ and RW peaks, the spectra show a broad feature ($S_2'$), whose dispersion is marked by bars in Fig. 1(b). The kinematics chosen for the new data yield a $S_3$ peak intensity exceeding that of the RW. The data agree very well with the DFPT
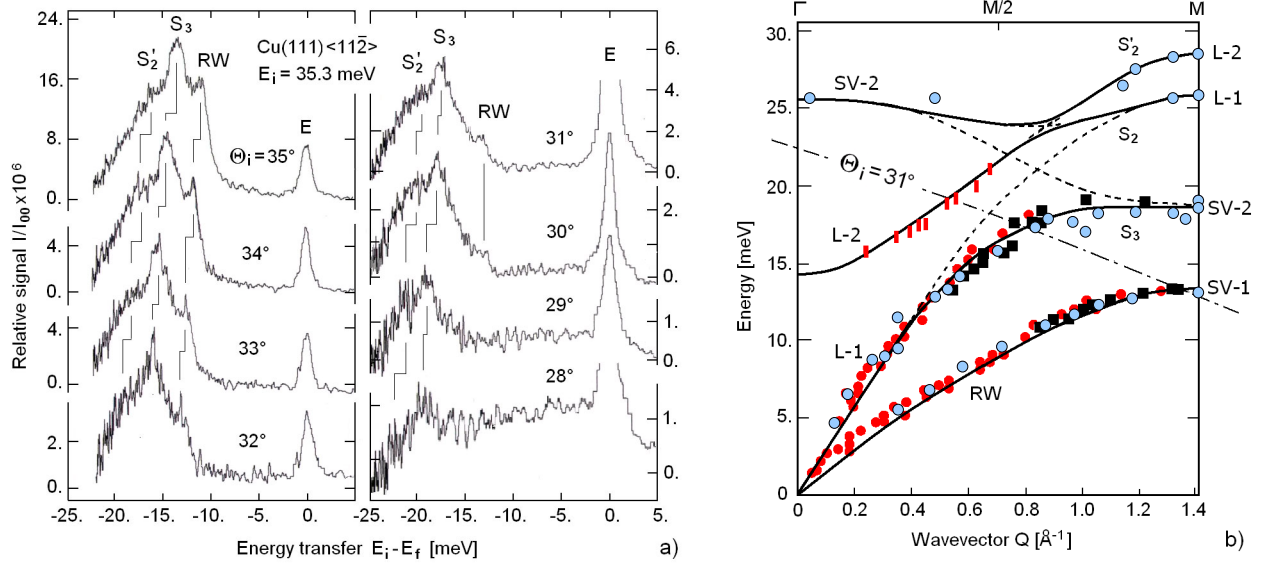
FIG. 1 (color online).    (a) A selection of HAS energy transfer spectra from Cu(111) along the $\langle 11\bar{2}\rangle$ direction at $T_s = 160$ K for an incident energy of 35.3 meV and incident angles $\Theta_i$. $E$ indicates the elastic peak. The $S_3$ resonance is the most prominent inelastic peak of the spectra, whereas the Rayleigh wave (RW) feature is weak and fades out at smaller $\Theta_i$. (b) Comparison of calculated dispersion curves with HAS (black squares: present; black (red) dots: from [5]), and EELS [6,7] (gray dots) data for the Cu(111) surface. The bars in (b) indicate the position of the $S'_2$ shoulder in the spectra (a) at higher energy. The intersections of the 31° scan curve (dash-dotted line) with the dispersion curves correspond to the phonon peaks appearing in the HAS spectrum at $\Theta_i = 31°$.

surface-phonon dispersion curves (full lines) obtained from the ridge lines of the calculated phonon densities of states (DOS) (Fig. 2) projected onto the first- and second-layer shear vertical (SV-1, SV-2) and longitudinal (L-1, L-2) components, respectively. The dashed lines in Fig. 1(b) illustrate the hybridization leading to avoided crossings of SV-2 and L-1 and L-2.

The surface-phonon dispersion curves and the phonon-induced SCD oscillations for some selected surface phonons have been calculated within DFPT [16], with ultrasoft pseudopotentials and a generalized gradient approximated exchange and correlation energy functional [17]. A plane wave basis with a 30 Ry energy cutoff for the wave functions and 480 Ry for the charge density has been used for a 25 layer slab with 13 Å of vacuum. The irreducible Surface Brillouin Zone (SBZ) was sampled over a $12 \times 12$ Monkhorst-Pack grid (19 **k**-points). The surface relaxation was determined by requiring that the forces were $<0.35$ meV/Å and found in reasonable agreement with experiments [18] and previous *ab initio* [19–21] and semiempirical calculations [22]. The interatomic force constants are calculated for bulk Cu and for a 7-layer Cu (111) slab. Then a 25-layer slab is constructed with the surface force constants taken from the 7-layer slab, and the inner atom force constants from the bulk [23]. The radial force constant between nearest neighbors in the surface plane turns out to be 11% softer than in the bulk.

The phonon dispersion curves and the projected phonon DOS as functions of energy and wave vector $Q$ have been

calculated for the $\bar{\Gamma}\bar{M}$ direction of the SBZ [23]. The calculated DOS shows the sharp ridge of RW for both SV-1 and SV-2 components, and a much weaker intensity in the L-1 and L-2 longitudinal components, as expected from the quasi-SV character of the RW. The DOS of Fig. 2 fully confirms early EAM results [9], e.g., the occurrence of two strong surface *optical* phonon resonances of SV and
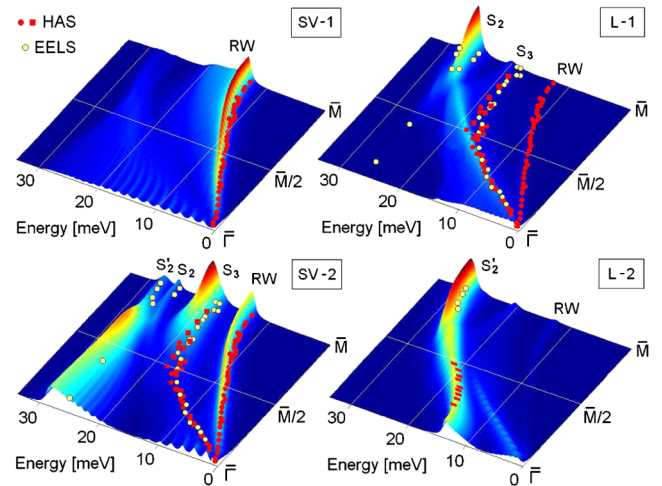


FIG. 2 (color online).   Calculated phonon DOS in the $\bar{\Gamma}\bar{M}$ direction projected onto the first layer for shear-vertical (SV-1) and longitudinal (L-1) polarizations, and onto the 2nd layer (SV-2 and L-2, respectively). The colored circles, squares, and bars are experimental data as given in the captions of Fig. 1.

longitudinal polarization, both localized in the 2nd layer
(Fig. 2, SV-2 and L-2). The longitudinal resonance in the
L-1 DOS apparently follows the band edge ending at $\bar{M}$ as
a gap mode ($S_2$). However, the avoided crossing between
SV-2 and L-1 at about 0.85 Å$^{-1}$ [Fig. 1(b)], with a gap of
6 meV, actually converts the surface acoustic longitudinal
mode into the $S_3$ resonance, in good agreement with both
HAS and EELS data. Whereas such intensity transfer from
L-1 to SV-2 is well understood for EELS data since elec-
trons penetrate sufficiently to give an appreciable scatter-
ing intensity also from 2nd-layer SV displacements, the
HAS intensities can only be explained through a calcula-
tion of the associated SCD oscillations. In this respect, we
note that previous *ab initio* calculations for Cu(111)
[25,26] and Cu(001) [27] have apparently not analyzed
2nd-layers resonances nor dynamic SCD oscillations.

The calculated SCD oscillations $\Delta n_\lambda(x, z)$ induced by
the phonon mode $\lambda = (\mathbf{Q}, j)$ ($j = \text{RW}, S_3$ for $\mathbf{Q} = \bar{M}$,
$\bar{M}/2$ and $j = S_2$ for $\mathbf{Q} = \bar{M}, \bar{\Gamma}$), are shown by means of
their contour lines in Fig. 3 corresponding to $\Delta n_\lambda = \pm(1, \frac{1}{2}, \frac{1}{4}, \ldots, \frac{1}{128}) \times 10^{-4}$ a.u.. Also shown are the static
profiles $z_t(x)$ of the surface at the turning point of He atoms
impinging either at $\Theta_i = 31°$ with $E_i = 35.3$ meV
(cf. Fig. 1) (broken line) or at room temperature ($E_i = 63$ meV) at normal incidence (full line). At these incident
energies, the corrugation of $z_t(x)$ is very small. The corre-
sponding charge density $n_t$ can be derived from Nyeland-
Toennies density-functional calculation of He-Cu repulsive
potential [28] as $n_t = E_i \cos^2\Theta_i/(326 \text{ eV} a_o^3)$ ($\sim 0.8 \times 10^{-4}$ a.u. in the experiments). The proportionality between
$E_i$ and $n_t$ implies that nonlinear corrections leading, e.g., to
anticorrugation effects in the static potential [29] are ne-
glected. The calculated static surface charge-density pro-
file as a function of the distance $z$ around the turning point
$z_t$ (cf. Fig. 3 in EPAPS [24]) is well represented by
$n(x, z) = n_t \exp[-(z - z_t)/\rho]$ with $\rho = 0.358$ Å, in good
agreement with the value 0.354 Å extrapolated from the
Nyeland-Toennies calculation [28]. Note that $n(x, z)$ de-
pends only weakly on $x$ via $z_t$. As appears from the almost
constant spacing of the contour lines (Fig. 3), also the SCD
oscillations $\Delta n_\lambda(x, z)$ decays exponentially (Fig. 3) with
decay lengths $\rho_\lambda \cong \rho$ and are therefore proportional to
$n(x, z)$. In general, the phonon-induced corrugation at the
turning point is given by $\Delta \zeta_\lambda(x, z_t) = \rho \Delta n_\lambda(x, z_t)/n_t$.
This, for instance, is about $3.2 \times 10^{-3}$ Å for the $S_3(\bar{M})$
mode under present experimental conditions. This ampli-
tude, which is twice smaller than for RW($\bar{M}$) and twice
bigger than for $S_2(\bar{M})$, is due to the SV displacements of
2nd-layer atoms. The same holds for $S_2(\bar{\Gamma})$. The dynamic
corrugation of $\bar{M}/2$ modes is comparable to that of
RW($\bar{M}$); it is noted however that the displacement fields
of the $\bar{M}/2$ modes depicted in Fig. 3 have a normalization
over the crystal volume which is half of that of $M$ modes,
and therefore their contributions are to be counted twice.
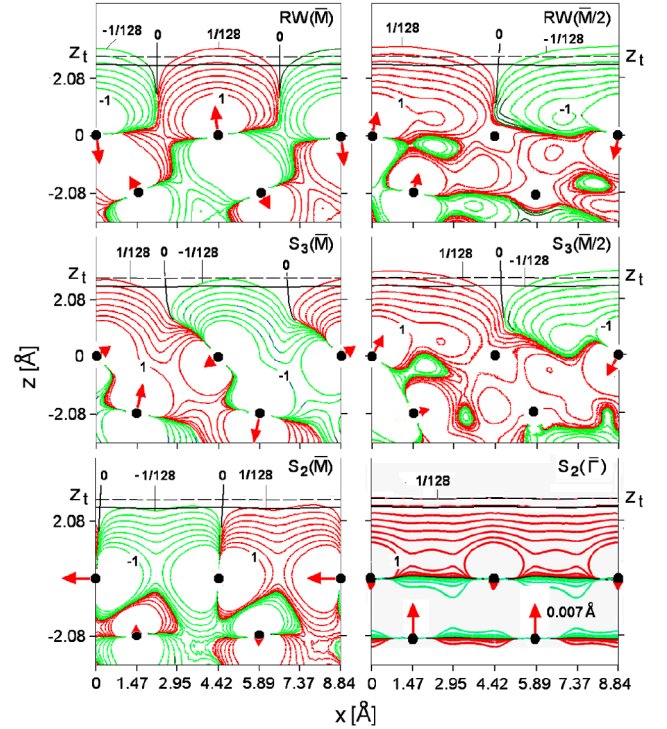The one-phonon HAS differential reflection coefficient



FIG. 3 (color online). Contour plots of the surface charge
density (SCD) modulation as a function of normal ($z$) and
parallel ($x$) coordinates, induced by frozen-phonon displace-
ments (arrows) of the atoms (dots) for the Rayleigh wave
(RW), the $S_3$ and $S_2$ modes at the point $\bar{M}$, for the RW and $S_3$
modes at the midpoint ($\bar{M}/2$) of $\bar{\Gamma}\bar{M}$ and for the $S_2$ mode at $\bar{\Gamma}$ [in
units of $10^{-4}$ a.u., from $\pm 1$ to $\pm 1/128$, each step dividing by 2,
with black (red) lines for positive modulations and gray (green)
lines for negative modulations]. The arrow length is proportional
to the displacement amplitude with the 2nd-layer $S_2(\bar{\Gamma})$ displace-
ment equal to 0.007 Å. The horizontal broken (full) lines indicate
the He turning points for an incident energy $E_i = 35.3$ meV
(63 meV) and angle $\Theta_i = 31°$ (0°). For the static SCD, see
Fig. 3 of additional material [24].

(DRC) in the approximation of very small surface corru-
gation [30] at $T = 0$ is expressed, up to Debye-Waller and
kinematic factors, by

$$\frac{d^2\mathfrak{R}^{(1)}}{dE_f d\Omega_f} \propto \sum_{\mathbf{Q}j} |\Delta k_z \Delta \zeta_j(\mathbf{Q}, z_t)|^2 \delta(E_i - E_f - E_{\mathbf{Q}j}), \quad (1)$$

where $\Omega_f$ is the final solid angle, $\Delta k_z$ is the normal wave
vector transfer in He scattering, $\Delta \zeta_j(\mathbf{Q}, z_t)$ is the 2D
Fourier transform of $\Delta \zeta_\lambda(x, z_t)$, and $E_{\mathbf{Q}j}$ the phonon en-
ergies. The contributions of the $S_3$ and RW modes to the
DRC for $E_i = 35.3$ meV and $\Theta_i = 31°$ when compared
with the phonon SV-1 DOS along the 31° scan curve
(Fig. 4, peaks vs heavy line) and to the experimental
spectrum [Fig. 1(a)], clearly prove that HAS spectroscopy
does not give the phonon amplitudes but the corresponding
SCD oscillations. It also appears that the HAS intensity of
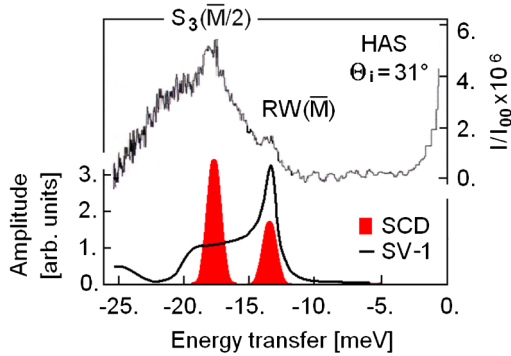$S_3$ measured below 31° comes more and more from the

FIG. 4 (color online).   Contributions of the $S_3$ and RW modes to the differential reflection coefficient for $E_i = 35.3$ meV and $\Theta_i = 31°$ (peaks) compared to the phonon SV-1 DOS along the $31°$ scan curve [Fig. 1(b)].

atomic SV displacements in the 2nd layer through the corresponding SCD modulation [31].

The present analysis can be extended to IETS. As shown by Lorente and Persson [32], the IETS differential conductivity as measured with a scanning tunneling microscope is proportional to the squared phonon-induced modulation of the surface electron density (Fermi-level electron DOS) at the tip apex. Thus, the large SCD oscillations associated with the SV-2 resonance are expected to strongly modulate the electron density at the tip apex. This might account, e.g., for the large 21 meV peak recently observed in IETS experiments on Cu(111) [15]. The role of SV-2 and L-2 resonances is also evident in Al(001), where recent DFPT calculations show a close matching within the main peaks of the Eliashberg function $\alpha^2 F(\omega)$ [33] and the DOS of the two 2nd-layer resonances [34]. It is argued that these properties are intrinsic to most metal surfaces where the anomalous resonance has been observed. The ability of HAS (and IETS as well) of detecting subsurface modes through their induced SCD oscillations can also provide a rich information on the dynamics of thin metal overlayers with a strong electron-phonon interaction, as argued, e.g., from HAS studies of Pb(111) overlayers on Ge(001) [35].

[1] H. Ibach and H. Lüth, *Solid-State Physics* (Springer-Verlag, Berlin, 1996), 2nd ed.
[2] M. Rocca, Landolt-Bornstein (2001), Vol. III/42.
[3] G. W. Farnell, in *Physical Acoustics*, edited by W. P. Mason and R. N. Thurston (Academic Press, New York, 1970), Vol. 6, p. 109.
[4] R. B. Doak, U. Harten, and J. P. Toennies, Phys. Rev. Lett. **51**, 578 (1983).
[5] U. Harten, J. P. Toennies, and Ch. Wöll, Faraday Discuss. Chem. Soc. **80**, 137 (1985).
[6] M. H. Mohamed *et al.*, Phys. Rev. B **37**, 2763 (1988).
[7] B. M. Hall *et al.*, Phys. Rev. B **38**, 5856 (1988).
[8] M. W. G. Ponje *et al.*, Phys. Rev. B **67**, 174301 (2003).
[9] J. S. Nelson *et al.*, Phys. Rev. B **40**, 1465 (1989).
[10] G. Benedek *et al.*, Phys. Rev. B **48**, 4917 (1993).
[11] P. Zeppenfeld *et al.*, Phys. Rev. B **38**, 12329 (1988).
[12] C. S. Jayanthi *et al.*, Phys. Rev. Lett. **59**, 795 (1987).
[13] C. Kaden *et al.*, Phys. Rev. B **46**, 13509 (1992).
[14] B. Hellsing, A. Eiguren, and E. V. Chulkov, J. Phys. Condens. Matter **14**, 5959 (2002).
[15] H. Gawronski, M. Mehlhorn, and K. Morgenstern, Science **319**, 930 (2008).
[16] S. Baroni *et al.*, Rev. Mod. Phys. **73**, 515 (2001).
[17] J. P. Perdew, K. Burke, and M. Ernzerhof, Phys. Rev. Lett. **77**, 3865 (1996).
[18] K. H. Chae, H. C. Lu, and T. Gustafsson, Phys. Rev. B **54**, 14082 (1996).
[19] K. P. Bohnen and K. M. Ho, Surf. Sci. Rep. **19**, 99 (1993).
[20] J. L. F. Da Silva, C. Stampfl, and M. Scheffler, Surf. Sci. **600**, 703 (2006).
[21] D. Hennig, M. V. Ganduglia-Pirovano, and M. Scheffler, Phys. Rev. B **53**, 10344 (1996).
[22] S. D. Borisova *et al.*, Phys. Rev. B **74**, 165412 (2006).
[23] Full set of dispersion curves is given in Fig. 1 of additional material [24]. A calculation for a 18-layer slab with no insertion of bulk planes gives essentially the same phonon structure (cf. Fig. 2 in additional materials [24]).
[24] See EPAPS Document No. E-PRLTAO-101-079846 for the additional material. These documents can be reached via a direct link in the online article's HTML reference section or via the EPAPS homepage (http://www.aip.org/pubservs/epaps.html).
[25] R. Heid and K.-P. Bohnen, Phys. Rep. **387**, 151 (2003).
[26] Y. Chen *et al.*, Phys. Rev. Lett. **70**, 603 (1993).
[27] A. dal Corso, Phys. Rev. B **64**, 235118 (2001).
[28] C. Nyeland and J. P. Toennies, Chem. Phys. **321**, 285 (2006).
[29] J. N. Jean *et al.*, Phys. Rev. Lett. **92**, 013201 (2004).
[30] V. Bortolani and A. C. Levi, Riv. Nuovo Cimento **9**, 1 (1986).
[31] It is worth noticing that the DOS for the SV-2 atomic motion (Fig. 2) is almost identical to the DOS of the multipolar oscillations in the first layer reported in Ref. [13].
[32] N. Lorente and M. Persson, Phys. Rev. Lett. **85**, 2997 (2000).
[33] I. Yu. Sklyadneva *et al.*, J. Phys. Condens. Matter **20**, 165203 (2008).
[34] V. Chis *et al.*, J. Phys. Condens. Matter **19**, 305011 (2007).
[35] L. Floreano *et al.*, Prog. Surf. Sci. **72**, 135 (2003).